Tracing biomass burning aerosol from South America to Troll Research Station, Antarctica

M. Fiebig,[1] C. R. Lunder,[2] and A. Stohl[1]

Received 5 April 2009; revised 19 May 2009; accepted 15 June 2009; published 25 July 2009.

[1] The atmospheric observatory at the Norwegian Research Station Troll in Queen Maud Land, Antarctica, holds, since February 2007, the first all-year Antarctic atmospheric aerosol particle number size distribution measurements. These are colocated with measurements of the aerosol absorption and spectral scattering coefficients. In June 2007, this instrument set observed an aerosol whose properties were indicative of a biomass burning aerosol. These properties included two log-normal size distribution modes with median particle diameters of 0.105 μm and 0.36 μm, sharply falling off to smaller and larger sizes, and peaks in scattering and absorption coefficient. With backward plume calculations of the Lagrangian transport model FLEXPART and the MODIS fire activity product, a source-receptor relationship was established between biomass burning events in Central Brazil and the aerosol seen at Troll. This is the first direct evidence that the Antarctic continent is susceptible to emissions from as far north as Southern tropical latitudes. **Citation:** Fiebig, M., C. R. Lunder, and A. Stohl (2009), Tracing biomass burning aerosol from South America to Troll Research Station, Antarctica, *Geophys. Res. Lett.*, *36*, L14815, doi:10.1029/2009GL038531.

1. Introduction

[2] Atmospheric aerosol burden in Antarctica attributed to long-range transported biomass burning emissions at lower Southern latitudes has been postulated in numerous studies over the past decade. Reporting from their first measurements of aerosol properties at South Pole, *Hansen et al.* [1988] find an annual cycle in the particulate black carbon (BC) concentration with a peak in austral summer and a minimum in winter. *Wolff and Cachier* [1998] confirm the annual cycle in the Antarctic airborne BC concentration, and attribute it at least partially to biomass burning in the Southern hemisphere by using an offline Lagrangian transport model. *Pereira et al.* [2006] tentatively connect a specific particulate BC peak measured in the Antarctic peninsula with South American biomass burning emissions using NCEP reanalysis windfields for that period.

[3] Using the first Antarctic all-year atmospheric aerosol particle number size distribution measurements, this case study will establish the first firm source-receptor relationship for biomass burning aerosol reaching Antarctica, i.e., the Norwegian Troll Research Station.

2. Location and Methods

[4] The Troll Research Station (TRS) is located in Queen Maud Land on the Antarctic continental shelf, about 220 km from the coast. Its closest neighbour stations are the South African SANAE IV station, 190 km east-north-east, and the German Neumeyer station, 420 km east-north-east of TRS. TRS is situated on snow-free bedrock and accessible by air-transport during Antarctic summer, facilitated by a blue-ice airfield on the glacier 7 km north of the main station. After TRS was turned from a summer into an all-year station in 2005, the Norwegian Institute for Air Research (NILU) deployed a container-housed atmospheric observatory (TRS-AO) in February 2007.

[5] A detailed description of TRS-AO, meteorological conditions, instrument set, and some first results can be found in *Hansen et al.* [2009]. TRS-AO is situated 150 m upwind in the main wind direction (from north-east) of the TRS main building. This location was a compromise for the early-development phase of TRS when surroundings further away were inaccessible in winter, and results in some contamination of the air sampled at TRS-AO by local sources (power generator, local vehicle traffic, sanitary system outgassing, fuel depot, etc.). Contaminated data is currently detected by wind direction and peaks in tracer species (new particle concentration) and flagged as influenced by local sources. TRS-AO will, in the near future, be moved to a location with little to no local contamination.

2.1. Experiment

[6] The instrument set at TRS-AO targeted at atmospheric aerosol properties comprises: 1) a multi-wavelength integrating nephelometer (TSI Inc., model 3563, measuring aerosol scattering and backscattering coefficient σ_{sp} and σ_{bsp} at wavelengths λ = 450, 550, 700 nm); 2) a single-wavelength particle soot absorption photometer (PSAP, custom built, principle, geometry, and filter material as described by *Bond et al.* [1999], measuring aerosol absorption coefficient σ_{ap}, λ = 523 nm); 3) a Differential Mobility Particle Sizer (DMPS, custom built, Vienna-type [*Reischl*, 1991], measuring particle number size distribution $dN/d\log D_p$ with diameters 20 nm < D_p < 800 nm); 4) a Precision Filter Radiometer (PFR, Global Atmosphere Watch version, measuring columnar aerosol optical depth, λ = 369, 412, 500, 862 nm); 5) a filter pack sampler (organic and inorganic chemical composition). Further instruments cover meteorological standard parameters (pressure, temperature, humidity, wind direction and velocity), all-sky images, UV irradiance (incl. ozone column), and the concentrations of

[1]Department for Atmospheric and Climate Research, Norwegian Institute for Air Research, Kjeller, Norway.
[2]Monitoring and Information Technology Department, Norwegian Institute for Air Research, Kjeller, Norway.

0094-8276/09/2009GL038531$05.00

gas-phase mercury, carbon monoxide, persistent organic pollutants, and other greenhouse gases.

[7] The present case study on aerosol transport focuses on the data of nephelometer, PSAP, and DMPS. All these instruments receive their sample through a common laminar flow, total suspended matter inlet. From the inlet main pipe (100 mm diameter), near-isokinetic take-offs lead to each instrument. For quality assurance, the nephelometer's zero point is updated twice per hour using particle free air, while its span is checked weekly by means of high purity carbon dioxide [*Anderson et al.*, 1996]. Owing to the background conditions at TRS with low total aerosol load, the nephelometer data are averaged to hourly values, which are corrected for angular truncation [*Anderson and Ogren*, 1998]. Similarly, the σ_{ap} values provided by the PSAP are averaged hourly, and corrected for the instrument's cross-sensitivity to particle scattering using the scheme of *Bond et al.* [1999]. For the DMPS system, the critical parameters (sample and sheath flow) are monitored weekly by the local technician. The raw size scans of the DMPS are inverted to particle size distributions using the inversion algorithm of *Fiebig et al.* [2005]. For the inversion, the DMPS transfer function of *Stolzenburg* [1988] and the particle charging efficiency of *Wiedensohler* [1988] are used.

2.2. Modelling

[8] To identify the source regions of the sampled air masses, we use 3-hourly backward simulations with the Lagrangian particle dispersion model FLEXPART [*Stohl et al.*, 1998, 2005] driven with 3-hourly operational analyses, both from the European Centre for Medium-Range Weather Forecasts and the National Center of Environmental Prediction (NCEP) Global Forecast System (GFS) model, with $1^\circ \times 1^\circ$ resolution. During every 3-hour interval, 200000 particles were released at the measurement point and followed backward in time for 30 days to calculate an emission sensitivity (ES) under the assumption that removal processes can be neglected. The ES (in units of s kg^{-1}) in a particular grid cell is proportional to the particle residence time in that cell and measures the simulated mixing ratio at the receptor that a source of unit strength (1 kg s^{-1}) in the cell would produce. The ES distribution in a 100 m footprint layer adjacent to the surface is particularly relevant because most of the emissions occur near ground.

[9] Daily fire detections from the MODIS instruments onboard the Aqua and Terra satellites [*Giglio et al.*, 2003] were used to locate active vegetation fires. Using the fire detections, information on land cover at 1 km resolution [*Hansen et al.*, 2000], and an algorithm recently described by *Stohl et al.* [2007], emissions of carbon monoxide (CO) were determined. By multiplying the FLEXPART footprint ES values with the fire emissions, CO source contribution maps and (by areal integration of these maps) time series of a biomass burning CO tracer at the Troll station were calculated.

3. Data and Discussion

[10] The case study discussed here concerns the period between 10 May and 28 June 2007 (days of year (DOY) 130–180). Figure 1 shows time series of the data provided by the ground-based aerosol in situ instruments at TRS-AO for this period, together with selected trace gas concentrations. Figure 1b shows the time series of boundary layer ozone (blue) and carbon monoxide (black, both hourly averages) as tracers for stratospheric air and combustion sources, respectively. Figure 1c depicts time series of the aerosol scattering coefficient $\sigma_{sp}(\lambda)$ at the three operating wavelengths of the nephelometer, while Figure 1d features time series of the aerosol absorption coefficient σ_{ap} and single scattering albedo ϖ_0 (ratio of scattering and extinction coefficient), both at 523 nm wavelength. The ϖ_0 values were calculated from 12 h averages of $\sigma_{sp}(\lambda)$ and σ_{ap} while interpolating $\sigma_{sp}(\lambda)$ geometrically to the PSAP wavelength, and only if both were not simultaneously smaller than their respective detection limit (0.1 Mm^{-1} and 0.5 Mm^{-1}). Figure 1e holds a colour contour plot of the particle size distribution time series in the particle diameter range 20–800 nm. Furthermore, Figure 1 uses hatched areas of various colours to depict time sequences where air masses can be attributed to specific origins using FLEXPART backward plume calculations or signatures in the data.

[11] Due to its current, temporary location, TRS-AO is at times influenced by activity at the TRS main building, including vehicle traffic (sequences hatched in red in Figure 1). These episodes are marked by peaks in the particle size distribution centred around $D_p \approx 0.045$ μm and inverse peaks in the single scattering albedo, but don't show much signature in the hourly averages of scattering coefficient and carbon monoxide. Air masses reaching TRS-AO via the free troposphere from lower latitudes as identified by FLEXPART (hatched in light blue) are characterised by overall low concentrations in the particle size distribution and values for scattering and absorption coefficient around the detection limit of the respective instruments. For the elevated concentrations close to the nucleation size range during these episodes, local contamination cannot be ruled out. Similarly to the free tropospheric pathway, air masses reaching TRS-AO through the planetary boundary layer (PBL) from the central Antarctic continent (hatched in green), where the air descended from the free troposphere or even tropopause region, show low overall particle loadings. However, central Antarctic air features a characteristic mode in the particle size distribution centred around $D_p \approx 0.07$ μm that may become dominant enough to cause an increase in the scattering coefficient above baseline values (DOY 162–164). This indicates more aerosol processing (gas-to-particle conversion, coagulation) since the last precipitation event in central Antarctic air than in free tropospheric air coming directly from lower latitudes. Marine air masses (hatched in dark blue) being transported to TRS-AO through the PBL from the continental shore characteristically show particle concentrations with $D_p > 0.3$ μm elevated above baseline level which are caused by sea spray and result in peaks in the scattering coefficient.

[12] The most prominent feature in Figure 1, however, and subject of this case study, is the peak in all displayed aerosol parameters between DOY 170 and 172. During this period, the particle size distribution is dominated by particles in the accumulation mode size range (0.1 μm $< D_p <$ 1.0 μm), and is comprised of two log-normal modes with integral particle number concentration (standard conditions, $T = 273.15$ K, $p = 1013$ hPa) $N_1 = 950$ cm^{-3}, median diameter $D_{med,1} = 0.105$ μm, and geometric standard

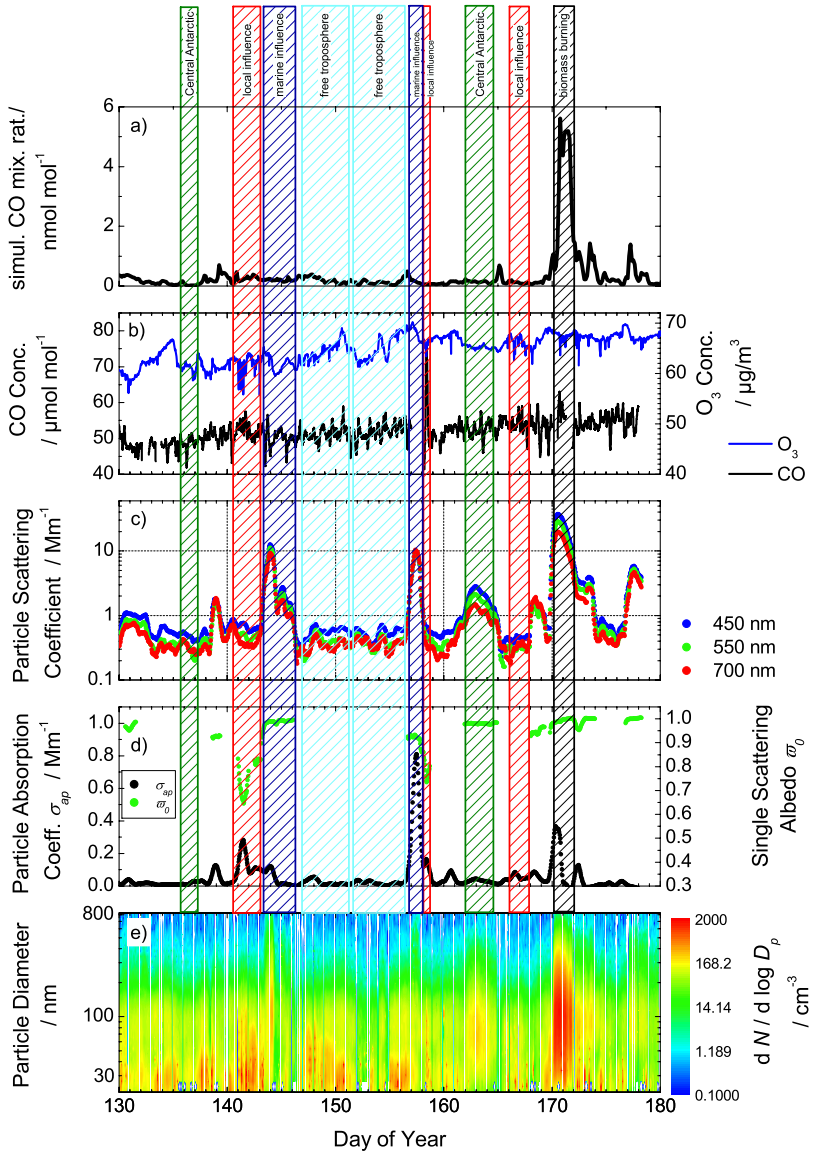

Figure 1. Assembled time series of data provided by ground based in situ aerosol instruments at TRS-AO, together with selected trace gas species, for the period of 10 May to 28 June 2007. (a) FLEXPART simulated forest fire CO concentration, (b) ozone and carbon monoxide, (c) spectral particle scattering coefficient σ_{sp}, (d) particle absorption coefficient σ_{ap}(523 nm) and single scattering albedo ϖ_0(523 nm) (shown only if σ_{sp} and σ_{ap} above detection limit), and (e) particle number size distribution.

deviation $\sigma_{g,1} = 1.7$ for the smaller mode, and $N_2 = 30$ cm^{-3}, $D_{med,1} = 0.360$ μm, and $\sigma_{g,1} = 1.4$ for the larger mode (see Figure 2). Over the period, the single scattering albedo ϖ_0 fluctuates around 0.98. The signature is much more readily to see in the aerosol particle properties than in the trace gas concentrations, where a small peak in the CO concentration is observed.

[13] The named properties of this aerosol, i.e. its particle size distribution being dominated by the accumulation mode with concentrations decreasing sharply to smaller and larger particle diameters, are characteristic of aerosols originating from biomass burning. As summarised in an overview by *Reid et al.* [2005b], the particle fraction of fresh smoke aerosol from a tropical forest fire has D_{med} values between 0.1 μm and 0.13 μm, and σ_g values between 1.68 and 1.77. For aged tropical forest fire smoke, values for D_{med} between 0.18 μm and 0.21 μm and from 1.55 to 1.65 for σ_g are stated, but D_{med} values as large as 0.34 μm, with a corresponding integral particle number concentration of $N = 250$ cm^{-3}, have been reported for a boreal forest fire plume that had aged 6–7 days [*Fiebig et al.*, 2003]. The single scattering albedo ϖ_0 varies between 0.74 for flaming combustion of tropical forest [*Reid et al.*, 2005a] and 0.90–0.98 for regional haze of African Savanna fires [*Formenti et al.*, 2003]. Irrespective that the detailed microphycical properties of biomass burning aerosol are a detailed function of fuel, size and type of burn (smoldering or flaming), occurrence of pyro-convective cloud processing, and dilution over the whole lifetime of the plume, all of which may even vary between different parts of the plume, this

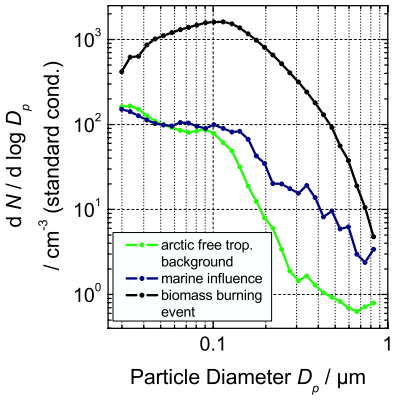

Figure 2. Representative particle number size distributions in marine, continental, and biomass burning aerosol at Troll, illustrating the unique features of biomass burning aerosol.

comparison indicates that the aerosol seen at TRS-AO would be a rather typical example of this aerosol type. This holds even for the total particle concentration, which is comparable in magnitude to the case reported by *Fiebig et al.* [2003] which had a similar age. It is also apparent that the signature of a biomass burning plume is more readily detected in the aerosol particle than in the trace gas properties. After long transport times, the signature in the trace gas concentrations has almost vanished due to dilution. The particle fraction has been diluted as well, but the signature is preserved in the shape of the particle size distribution. Gas-to-particle conversion and cloud processing under transport would act almost exclusively on the pre-existing and dominating accumulation mode aerosol, but increase its particle size only slowly, thus preventing formation of particles outside this size range.

[14] The microphysical and optical properties alone would be a strong indication that the discussed aerosol observed at TRS-AO is a biomass burning aerosol. To make the case complete, FLEXPART was used in its backward plume mode in order to establish a source-receptor connection. Figure 3 shows a map of the column integrated emission sensitivity of the air mass arriving at TRS-AO on 21 June, 2007, 03:00 UTC, based on the GFS meteorological data. The map also includes all fire hot spots detected by MODIS in grid cells with non-zero emission sensitivity (black: grassland fire; red: forest fire). The map shows that the backward plume separates into several branches 3–4 days before arrival at TRS-AO. The northernmost branch turns westward toward South America, and spreads into a large, but well-defined catchment area that covers Central Brazil. A corresponding footprint emission sensitivity map (not shown) yields that the air indeed had surface contact in this area. Calculations using the alternative ECMWF meteorological data showed slightly less influence from the burning and a few hours earlier, but were otherwise consistent with the GFS results shown. The same catchment area is subject to extended biomass burning activity, both forest and grassland fires, in the period of interest. It is thus safe to conclude that the aerosol observed at TRS-AO on DOY 170–172 of 2007 was indeed a biomass burning aerosol originating from Central Brazil, reaching TRS-AO about 11–12 days after emission.

4. Conclusion and Outlook

[15] For the first time, a firm source-receptor connection for the episodic transport of biomass burning aerosol from tropical latitudes (Central Brazil) to Antarctica (TRS-AO) is established by investigation of a transport case that occurred in the Antarctic winter 2007 (19–20 June). To this aim, measurements of the aerosol particle number size distribution (part of the first Antarctic all-year measurements of this property, started February 20007 and continued to date) are combined with backward plume calculations of the Lagrangian transport model FLEXPART. The timing of the observations coincides with the peak of the biomass burning season in Brazil. This study confirms earlier indication of biomass burning emissions reaching Antarctica, and establishes that even tropical emissions may reach the Antarctic continent. Different from the northern hemisphere where the most significant anthropogenic pollution sources influencing the Arctic are located at mid- and high-latitudes, even tropical latitude emissions have a measurable influence on the polar region in the southern hemisphere. Even though anthropogenic emissions are naturally limited in the southern hemisphere due to the limited extent of land mass, care should be exercised since increasing southern hemisphere anthropogenic emissions may trigger similar adverse effects as observed in the Arctic.

[16] Since this cross-hemispheric transport event was observed already in the first winter of aerosol particle size distribution and aerosol optical property measurements at TRS-AO, indicating that such events may occur more often in southern winter than previously thought, future work will focus on establishing a transport climatology of biomass burning emissions into Antarctica based on data obtained at TRS-AO.

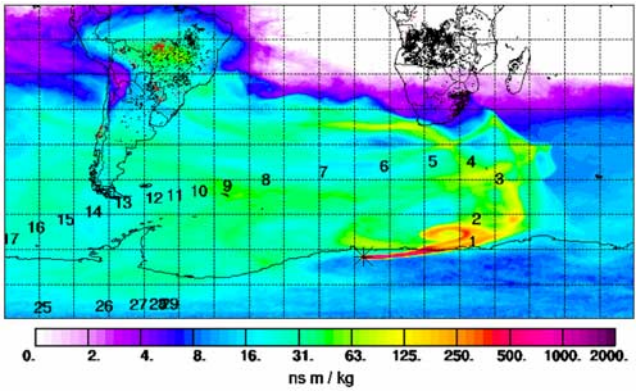

Figure 3. Map of column integrated emission sensitivity of air masses arriving at TRS on 21 June 2007 (day of year 171) 03:00 UTC, using backward calculation with the Lagrangian transport model FLEXPART, based on GFS meteorological data. The numbers indicate the plume's centre of gravity at the stated number of days backward in time. Also depicted are forest and agricultural fire hot-spots as obtained by combining the MODIS fire detection and land use maps.

[17] **Acknowledgments.** The authors thank the Norwegian Research Council for financial support of the Troll project and the Norwegian Polar Institute, including the 2007 overwintering team at Troll, for good collaboration and support in operating the observatory, also the instrument technicians at NILU for their continuous support, here in particular Jan Henrik Wasseng. The transport modelling work was supported by the Norwegian Research Council in the framework of the POLARCAT project. Further thanks go to Johan Ström (Institute for Applied Environmental Sciences, University of Stockholm) for supplying parts of the instrumentation.

References

Anderson, T. L., and J. A. Ogren (1998), Determining aerosol radiative properties using the TSI 3563 integrating nephelometer, *Aerosol Sci. Technol.*, *29*, 57–69.

Anderson, T. L., et al. (1996), Performace characteristics of a high-sensitivity, three-wavelength, total scatter/backscatter nephelometer, *J. Atmos. Oceanic Technol.*, *13*, 967–986.

Bond, T. C., T. L. Anderson, and D. Campbell (1999), Calibration and intercomparison of filter-based measurements of visible light absorption by aerosols, *Aerosol Sci. Technol.*, *30*, 582–600.

Fiebig, M., A. Stohl, M. Wendisch, S. Eckhardt, and A. Petzold (2003), Dependence of solar radiative forcing of forest fire aerosol on aging and state of mixture, *Atmos. Chem. Phys.*, *3*, 881–891.

Fiebig, M., C. Stein, F. Schröder, P. Feldpausch, and A. Petzold (2005), Inversion of data containing information on the aerosol particle size distribution using multiple instruments, *J. Aerosol. Sci.*, *36*, 1353–1372.

Formenti, P., W. Elbert, W. Maenhaut, J. Haywood, S. Osborne, and M. O. Andreae (2003), Inorganic and carbonaceous aerosols during the Southern African Regional Science Initiative (SAFARI 2000) experiment: Chemical characteristics, physical properties, and emission data for smoke from African biomass burning, *J. Geophys. Res.*, *108*(D13), 8488, doi:10.1029/2002JD002408.

Giglio, L., J. Descloitres, C. O. Justice, and Y. Kaufman (2003), An enhanced contextual fire detection algorithm for MODIS, *Remote Sens. Environ.*, *87*, 273–282.

Hansen, A. D. A., B. A. Bodhaine, E. G. Dutton, and R. C. Schnell (1988), Aerosol black carbon measurements at the south pole: Initial results, 1986–1987, *Geophys. Res. Lett.*, *15*, 1193–1196.

Hansen, G., et al. (2009), Atmospheric monitoring at the Norwegian Antarctic station Troll: Measurement programme and first results, *Polar Res.*, in press.

Hansen, M., R. DeFries, J. R. G. Townshend, and R. Sohlberg (2000), Global land cover classification at 1 km resolution using a decision tree classifier, *Int. J. Remote Sens.*, *21*, 1331–1365.

Pereira, E. B., H. Evangelista, K. C. D. Pereira, I. F. A. Cavalcanti, and A. W. Setzer (2006), Apportionment of black carbon in the South Shetland Islands, Antarctic Peninsula, *J. Geophys. Res.*, *111*, D03303, doi:10.1029/2005JD006086.

Reid, J. S., T. F. Eck, S. A. Christopher, R. Koppmann, O. Dubovik, D. P. Eleuterio, B. N. Holben, E. A. Reid, and J. Zhang (2005a), A review of biomass burning emissions part III: Intensive optical properties of biomass burning particles, *Atmos. Chem. Phys.*, *5*, 827–849.

Reid, J. S., R. Koppmann, T. F. Eck, and D. P. Eleuterio (2005b), A review of biomass burning emissions part II: Intensive physical properties of biomass burning particles, *Atmos. Chem. Phys.*, *5*, 799–825.

Reischl, G. P. (1991), Measurement of ambient aerosols by the differential mobility analyzer method: Concepts and realization criteria for the size range between 2 and 500 nm, *Aerosol Sci. Technol.*, *14*, 5–24.

Stohl, A., M. Hittenberger, and G. Wotawa (1998), Validation of the Lagrangian particle dispersion model flexpart against large scale tracer experiment data, *Atmos. Environ.*, *32*, 4245–4264.

Stohl, A., C. Forster, A. Frank, P. Seibert, and G. Wotawa (2005), Technical note: The Lagrangian particle dispersion model flexpart version 6.2, *Atmos. Chem. Phys.*, *5*, 2461–2474.

Stohl, A., et al. (2007), Arctic smoke: Record high air pollution levels in the European Arctic due to agricultural fires in eastern Europe, *Atmos. Chem. Phys.*, *7*, 511–534.

Stolzenburg, M. R. (1988), An ultrafine aerosol size distribution measuring system, Ph.D. thesis, Mech. Eng. Dep., Univ. of Minn.–Twin Cities, Minneapolis.

Wiedensohler, A. (1988), An approximation of the bipolar charge distribution for particles in the submicron size range, *J. Aerosol Sci.*, *19*, 387–389.

Wolff, E. W., and H. Cachier (1998), Concentrations and seasonal cycle of black carbon in aerosol at a coastal Antarctic station, *J. Geophys. Res.*, *103*, 11,033–11,041.

M. Fiebig and A. Stohl, Department for Atmospheric and Climate Research, Norwegian Institute for Air Research, Instituttveien 18, N-2007 Kjeller, Norway. (markus.fiebig@nilu.no; andreas.stohl@nilu.no)

C. R. Lunder, Monitoring and Information Technology Department, Norwegian Institute for Air Research, Instituttveien 18, N-2007 Kjeller, Norway. (chris.lunder@nilu.no)